ISSN : 0974 - 7435 Volume 8 Issue 5

BioTechnology
An Indian Journal

FULL PAPER

BTAIJ, 8(5), 2013 [714-720]

Automated classification of FDG-PET images combining voxels of interest and neuropsychological assessments

Wenlu Yang[1]*, Xiaoman Zhang[1], Fangyu He[1], Xudong Huang[2]
[1]Department of Electronic Engineering, College of Information Engineering, Shanghai Mritime University, Shanghai, 201306, (CHINA)
[2]Department of Department of Radiology, Brigham and Women's Hospital and, Harvard Medical School, Boston, MA 02115, (USA)
E-mail : wlyang@shmtu.edu.cn

ABSTRACT

To perform the automated classification of AD or MCI subjects vs. healthy control (HC) subjects from ADNI PET images database, the study presents a novel systematic method of combining voxels of interest in positron emission tomography (PET) images and the neuropsychological assessments of subjects. It aimes to find the appropriate technology for the early detection of Alzheimer's disease (AD) or mild cognitive impairment(MCI). The method includes four steps: pre-processing, extracting independent components using ICA, selecting voxels of interest, and classifying them using a Support Vector Machine (SVM) classifier. PET image data were obtained from the ADNI database including 91 HC, 50 patients with baseline diagnosis of AD and 105 patients with a baseline diagnosis of MCI. As a result, we achieved an excellent discrimination between AD patients and HC (accuracy 97.5\%, sensitivity 93.5\%, specificity 99.7\%), and a good discrimination between MCI patients and HC (accuracy 94.5\%, sensitivity 92.7\%, specificity 96.5\%). The experimental results showed that the proposed method can successfully distinguish AD or MCI from HC and that it is suitable for the automated classification of PET images. © 2013 Trade Science Inc. - INDIA

KEYWORDS

Alzheimer's disease;
Mild cognitive impairment;
Positron Emission Tomography;
Independent component analysis;
Support vector machine.

INTRODUCTION

Alzheimer's disease (AD) is the most common form of dementia, accounting for 60% to 80% of dementia cases[1], in the ageing population of today. The two major pathological hallmarks of AD are extracellular plaques and intracellular tangles. Other characteristics of AD are synaptic loss and neuronal cell death, leading to brain atrophy. Originally defined in 1999, mild cognitive impairment (MCI), a condition in which subjects are usually only mildly impaired in memory with relative preservation of other cognitive domains and functional activities and do not meet the criteria for dementia[2], or as the prodromal state AD[3]

To clinically diagnose AD or MCI patients at an early stage, many biomedical imaging techniques have

been used, such as structural and functional magnetic resonance imaging (sMRI)[1, 4], and positron emission tomography (PET)[5-7]. However, magnetic resonance imaging is performed in the evaluation of patients who have been suspected early AD, but this imaging study is neither sensitive nor specific for the diagnosis, whereas, PET imaging of ^{18}F-2-fluoro-2-deoxy-d-glucose (FDG) is demonstrated to be accurate and specific in the early detection of AD[7-9]. As a kind of function imaging, FDG-PET images can display lesions distribution of AD through the glucose metabolism in brain, directly reflect lesions of specific areas and the metabolic features, to diagnose and identify AD. Relative to other imaging, PET imaging has unique advantages in early diagnosis of AD[9]. However, how to deal with PET images, how to extract rich information containing in PET images, and how to classify the useful information extracting from PET images, have become a focus of attention.

Despite these useful imaging techniques, early treatment of AD still remains a challenge because valuation of these images normally depends on manual reorientation, visual reading and semiquantitative analysis[10]. So several methods have been proposed in the literature aiming at providing an automatic tool that guides the clinician in the AD diagnosis process[11-13]. These methods can be classified into two categories: mono-variate and multivariate methods. Statistical parametric mapping (SPM)[14] is a mono-variate method, consisting of doing a voxel-wise statistical test and inference, with comparing the values of the image under study to the mean values of the group of normal images[12]. This method suffers mainly from the well-known small sample size problem, that is, the number of available samples is much lower than the number of features used in the training step. By contrast, independent component analysis (ICA) is a multivariate analysis method, a significant kind of blind signal separation, and has already been applied to structural[11, 13] and functional brain images[15, 16]. It is also able to probe into PET datasets to provide useful information about the relationships among voxels. In order to distinguish AD and health controls (HC), support vector machine (SVM), a non-linear diagnostic tool, has received more attention[13, 17, 18]. In the current study, we proposed a novel approach for automatic classification of PET images, which includes four steps: preprocessing using SPM, extracting features by ICA, selecting voxels of interest, and classification of AD vs healthy controls using SVM.

MATERIALS AND METHODS

The framework of the proposed method was shown in Figure 1. We would explain it in detail in the following sections. Generally, the framework included five steps: pre-processing, extracting independent components using ICA and selecting voxel of interest (VOI), constructing feature matrix with ICs/CM (Clinical Measures), and classifying using a SVM classifier that was shown in Figure 1.

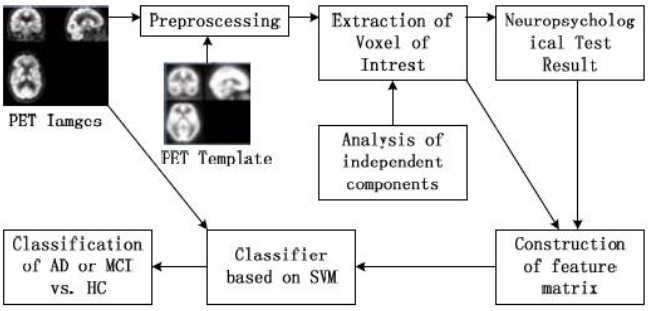

Figure 1: The framework of the proposed method.

Experimental PET data

The FDG-PET data used in the preparation of the study was obtained from the Alzheimer's Disease Neuroimaging Initiative (ADNI) database (www.loni.ucla.edu/ADNI/). The primary goal of the ADNI has been to test whether serial MRI, PET, other biological markers, and clinical and neuropsychological assessments can be combined to measure the progression of MCI and early AD. ADNI had recruited 800 adults, aged in the range from 55 to 90, to participate in the research - approximately 200 cognitively normal older individuals to be followed for 3 years, 400 people with MCI to be followed for 3 years, and 200 people with early AD to be followed for 2 years[4].

Selecting some images which contained similar protocol, we used baseline FDG-PET scans from 246 ADNI subjects, including 50 AD patients, 105 MCI patients and 91 healthy subjects, whose group-wise characteristics of the data set were showed in TABLE 1.

Preprocessing

FDG-PET scans were acquired according to a series of standardized protocols. The images were simply

FULL PAPER

TABLE 1 : The characteristics of the data set

Group	AD	MCI	HC
No.of subj.	50	105	91
M/F	20/30	35/70	40/51
Age	75.6±7.5	75.3±7.1	76.4±5.1
NPI-Q	3.9±3.5	1.8±2.5	0.5±0.9
FAQ	13.4±6.9	3.5±3.9	0.5±2.2

NPI-Q: Neuropsychiatric Inventory-Questionnaire; FAQ: Function Assessment Questionnaire.

preprocessed using Matlab toolbox SPM8[20]. Firstly, selecting a group of PET images, then all the images in the group were realigned to the first image, making sure that all of them were consistent with each other in the spatial atlas. At last those output realigned images were normalized to a standard template PET built in SPM8. In this specific process, each image was resliced and voxel volume was set to be 2 x 2 x 2mm^3.

Independent components analysis

To search for the source images that implied the underlying features of PET images, obviously a blind source separation problem, independent component analysis[13, 21, 22] was then brought into use. ICA can be stated as follows: let **X** be an observed random vector and **A** an unknown full rank mixing matrix such that: **X=AS**, shown in Figure 2, where the source signals **S** denotes latent sources. For application to PET images, each row of matrix **X** is the voxel values vectorized from one PET image out of *N*, the number of subjects. After the decomposition, a mixing matrix **A** and a source matrix **S** come into being. Each of the *K* columns of **A** can be figured as one component composite of information from all FDG-PET images and each of the *K* rows of **S** with the same number of voxels in one specific PET image can be used to realize the visualization of the component.

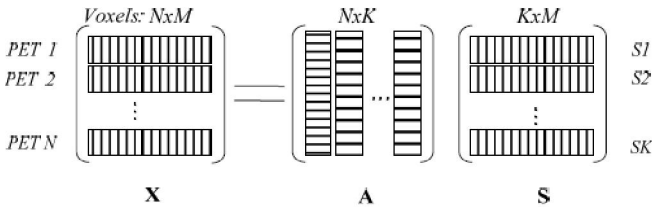

Figure 2 : ICA model for PET images. Here *N* means the number of subjects. Similarly *K* is the number of independent components and *M* denotes the number of voxels after preprocessing.

Moreover, we can select the voxels within the region of each independent component for all FDG-PET images involved. In order to extract features of each group of subjects, we thought about considering the voxel information in each source area. A common sense was that AD and MCI patients suffered from much more atrophied brain structures compared to healthy controls with similar background information. Research also showed that the patients with MCI suffered from glucose metabolism reducing, so the decision was made that the space area of each independent component would be mapped into every subject, then count the numbers of the voxels whose value indicated as brain structure parts.

Here since images of different subjects were already divided into two specific groups, named AD or MCI and HC, we might as well take each group as a session, a term broadly used in medical images acquisition. And then, all images belonged to these two groups were processed by a toolbox GroupICA[23], which was actually used to find out the independent components that can significantly differentiate the subjects belonging to a certain group. The program package GIFT built in GroupICA was used to find the diversity between groups, including three steps: Constructing grouping model and setting the analysis parameters, executing independent component analysis, and expanding independent component analysis results. After the whole analysis, five significant independent components were also shown in Figures 3 and 4.

As shown in Figures 3 and 5, five independent components were illustrated. The number in range of {27, …, -30} denoted the index of slices of a PET image. Each independent component was mapped back into the original PET images in the same space. It was easily observed that each independent component with a different color was mapped into a different area by voxels in the original PET images. If an area by voxels in images was much different between AD or MCI and HC subjects, the corresponding independent components covering the area were potentially important. In other words, these independent components would perform better in discriminating AD or MCI subjects from HC ones.

What's more, at a very early stage, AD or MCI patients may have appeared selective brain regions of

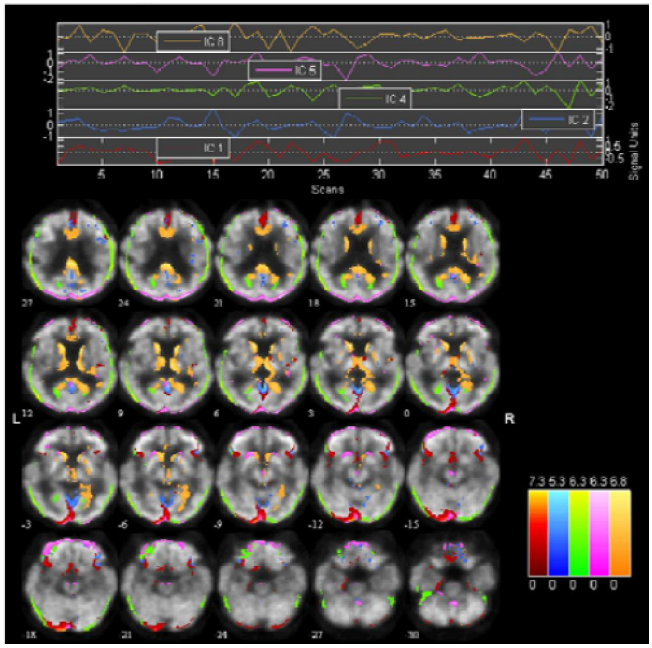

Figure 3 : The visualization of significant ICs of AD vs HC. From left to right of the legend: component 1; component 2; component 4; component 5; component 8.

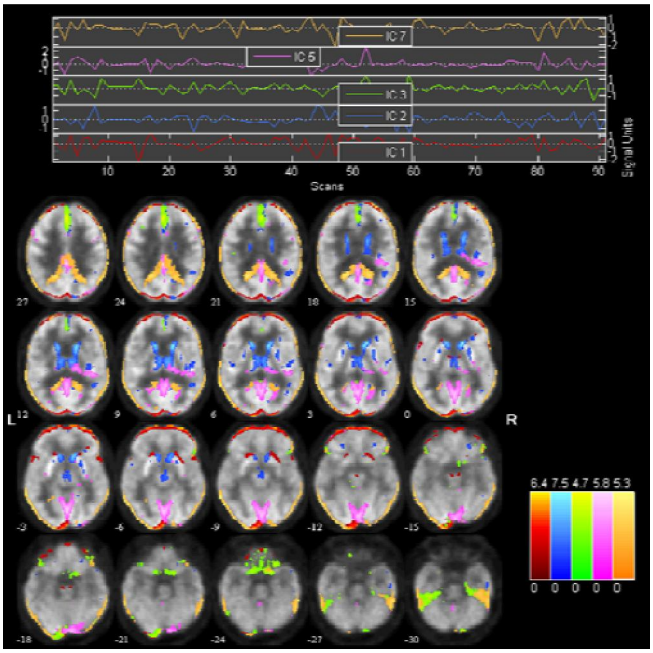

Figure 4 : The visualization of significant ICs of MCI vs HC. Different colors represent different sources. From left to right of the legend: component 1; component 2; component 3; component 5; component 7.

reduced energy metabolism. Although at this time the clinical symptoms, the cortical atrophy and neural psychology defect, have not yet appeared, at the same time the degree of local metabolic changes in FDG-PET images is related to the neuropsychological assessments of subjects. Therefore, we tried to take into account the neuropsychological assessments (NA) of subjects when we made the classification experiments. Out of NTR, Function Assessment Questionnaire(FAQ) and Neuropsychiatric Inventory-Questionnaire(NPI-Q) would have been added to the K-column matrix as the additional features. So the feature matrix now was consist of the voxels of interest and/or the neuropsychological assessments of subjects, and all the features that can also be used for classification.

Classification

The goal of this research was to better classify subjects from different groups from each other with an acceptable feature matrix. Since we have constructed a feature matrix in the foregoing procedures, we next would focus on classification of subjects involved in the research. We applied a Support Vector Machine (SVM) classifier using LIBSVM (http://www.csie.ntu.edu.tw/~cjlin/libsvm/) developed by Chih-JenLin of the National Taiwan University[24]. Support vector machine (SVM) is one of very popular classifiers and recently has been used to help distinguish AD subjects from elderly control subjects using anatomical MR imaging (MRI)[13, 17]. SVM conceptually implements the idea that vectors are nonlinearly mapped to a very high dimension feature space. In this feature space, a linear separation surface is created to separate the training data by minimizing the margin between the vectors of the two classes. SVM separates a given set of binary labeled training data with a hyperplane that is maximally distant from the two classes. Since it is impossible that real-world data would be linearly separable, we applied a soft-margin formulation of the SVM as a trade-off between maximizing the margin and minimizing the training error.

While performing classification, we assigned +1 as the label value for the group AD or MCI PET images and -1 for the group HC ones. Then we scaled all features by a column into the range of from -1 to 1. Taking the influence of the number of training samples on classification accuracy into account, all the images were randomly divided into two groups: 50% of the subjects randomly selected for training, and the rest for testing. Then we repeated the experiment over one hundred times. Finally, the averaged accuracy, sensitivity and

FULL PAPER

specificity were evaluated.

RESULTS

Extraction of independent components

The PET images of this experiment are 3D images of size M = 79 x 95 x 68 mm^3 voxels. Each voxel represents a brain volume of 2 x 2 x 2mm^3. Every row of the source matrix was reshaped into a 3D image called a map[19]. The Infomax ICA algorithm built in the toolbox GroupICA was then used to decompose the brain images, we can obtain independent components (ICs). We then compared the images between the group MCI and group HC in the same way. The results were explained as follows. In the experiment between group AD and group HC, the number of IC analyzed under the previous estimation was eight, and we made the visualization of the five available components: component 1, component 2, component 4, component 5, component 8, as is shown in Figure 3, which are the five significant ICs obtained by the toolbox GIFT. In the experiment between group MCI and group HC, the number of Ics analyzed under the previous estimation was seven, and we made the visualization of the five available components: component 1, component 2, component 3, component 5, component 7, as is shown in Figure 4, which are the five significant ICs obtained by the toolbox GIFT. The different color blocks represent different ICs in this figure. To get more in-depth biochemical information of these sources, we transformed the coordinates of these two significant sources to the coordinates of the standard space of Talairach and Tournoux[25] using the Matlab conversion program developed by Mathew Brett. The output Talairach and Tournoux coordinates of voxels were entered into TD client[25] which was created and developed by Jack Lancaster and Peter Fox. It is a high-speed database server for querying and retrieving data about human brain structure over the Internet (www.talairach.org). The detailed Talairach labels of IC sources are listed in TABLE 2. The left column in TABLE 2 is the source areas of the component, while the right column is the corresponding Brodmann area.

TABLE 2 : Talairach Lables of Ics

AD-HC	
Source 2 area	**Brodmann area**
Paracentral Lobule	4,5,6,31
Precuneus	7
Middle Frontal Gyrus	6,32
Superior Frontal Gyrus	6
Postcentral Gyrus	5
Precentral Gyrus	4
Cingulate Gyrus	31,32
MCI-HC	
Source 3 area	**Brodmann area**
Superior Frontal Gyrus	6
Medial Frontal Gyrus	6,8,32
Precentral Gyrus	4,6
Cingulate Gyrus	32
Postcentral Gyrus	3
Paracentral Lobule	5,6,31
Middle Frontal Gyrus	6
Precuneus	7

Classification

In this section, we randomly selected 50% of the samples to do training after we gained the feature matrix. For the randomness of the training samples, we get different results of the experiment. Therefore, we consider how to classify the samples many times to obtain the statistically averaged values. In the experiment, we repeated the classification 100 times and obtained the corresponding statistically averaged values. TABLE 3 shows the classification results with the different feature matrix.

TABLE 3 : Classification results of AD or MCI from HC (mean±sd%)

Training Sets	Parameter	AD vs HC	MCI vs HC
Only NA	Accuracy	88.4±3.9	79.7±3.2
	Sensitivity	90.4±6.5	77.0±7.5
	Specificity	86.7±6.5	83.0±6.1
Only ICs	Accuracy	91.6±2.2	90.0±2.3
	Sensitivity	76.5±6.0	81.9±4.4
	Specificity	99.8±1.3	99.4±1.5
ICs+NA	Accuracy	97.5±1.3	94.5±2.4
	Sensitivity	93.5±3.6	92.7±4.5
	Specificity	99.7±1.1	96.5±3.4

Three parameters that measure the results of the classification are: the Accuracy, the Sensitivity, and the Specificity, which can be described as Accuracy =

(Tp+Tn)/(Tp+Tn+Fp+Fn), Sensitivity = Tp/(Tp+Fp), and Specificity = Tn/(Tn+Fn), where Tp, Tn, Fp and Fn indicate true positives, true negatives, false positives and false negatives, respectively.

From the TABLE 3, it was easily found that the classifying results with both ICs and NA were better than that with only ICs or NA. The results demonstrated that the ICs extracted by the ICA-based method was able to effectively help NA improve the performance of diagnosis or classification of AD or MCI from HC PET images.

DISCUSSIONS AND CONCLUSIONS

In the study we had demonstrated that the fully automatic method based on ICA for the classification of PET images was very useful in discriminating among AD or MCI and HC subjects.

ICA is one of the data-driven, multivariate, and unsupervised methods with an advantage of using no a priori information. It has become an increasing popular biomedical data-mining technique as well as processing method for functional brain images. ICA might also be a useful tool for early AD diagnosis of PET images analysis because it has shown its usefulness in the processing PET images of schizophrenia patients. Therefore, in this study, we have applied ICA to the analysis of AD- and MCI-related PET images.

Experimental results on PET images from the ADNI databases have indicated that the proposed method based on ICA is a useful tool for classifying AD or MCI and HC image data.

Our results are also comparable with other related studies. Illan et al.[11] proposed an approach that included three steps: training, cross-validation by means of the leave-one-out method, and testing. They applied SVM based on a RBF kernel to obtain a classification accuracy of 88.2% by extracting features with PCA and 87.1% by ICA. Salas-Gonsalez et al.[26] developed an automated procedure to classify AD patients from FDG-PET data using a t-test to select voxels of interest and factor analysis to reduce feature dimension. They discriminated between AD/MCI and HC with sensitivity, specificity, and accuracy of 91.2%/98.1%, 80.8%/92.5%, and 88.0%/95.2%, respectively.

In the study, we had proposed an efficient method for distinguishing AD or MCI from HC. The method combining feature extraction, feature selection and classification techniques had been deeply studied and tested on a real PET database with promising results, and it can also be extended to other imaging modalities such as structural MR or fMRI. In the future, we will apply the proposed method to research on diagnosis of AD or MCI subjects based on multi-modality data, including structural MR images, PET images, fMRI images, and other imaging data.

ACKNOWLEDGMENT

The authors would like to express their gratitude for the paper supported by Innovation Program of Shanghai Municipal Education Commission (12YZ116), and for the experimental data from the Alzheimer's Disease Neuroimaging Initiative.

REFERENCES

[1] M.W.Weiner, D.P.Veitch, P.S.Aisen, L.A.Beckett, N.J.Cairns, R.C.Green, D.Harvey, C.R.Jack, W.Jagust, E.Liu, J.C.Morris, R.C.Petersen, A.J.Saykin, M.E.Schmidt, L.Shaw, J.A.Siuciak, H.Soares, A.W.Toga, J.Q.Trojanowski; Alzheimer's & dementia, **8**, S1 **(2012)**.

[2] R.C.Petersen, P.S.Aisen, L.A.Beckett, M.C.Donohue, A.C.Gamst, D.J.Harvey, C.R.Jack, W.J.Jagust, L.M.Shaw, A.W.Toga, J.Q.Trojanowski, M.W.Weiner; Neurology, **74**, 201 **(2010)**.

[3] B.Dubois, H.H.Feldman, C.Jacova, J.L.Cummings, S.T.Dekosky, P.Barberger-Gateau, A.Delacourte, G.Frisoni, N.C.Fox, D.Galasko, S.Gauthier, H.Hampel, G.A.Jicha, K.Meguro, J.O'Brien, F.Pasquier, P.Robert, M.Rossor, S.Salloway, M.Sarazin, L.C.deSouza, Y.Stern, P.J.Visser, P.Scheltens; Lancet Neurol, **9**, 1118 **(2010)**.

[4] C.R.Jack, M.A.Bernstein, N.C.Fox, P.Thompson, G.Alexander; Journal of Magnetic Resonance Imaging, **27(4)**, 685 **(2008)**.

[5] J.Chew, D.H.S.Silverman; The Medical clinics of North America, **97(3)**, 485 **(2013)**.

[6] Y.Yuan, Z.X.Gu, W.S.Wei; American Journal of Neuroradiology, **30(2)**, 404 **(2009)**.

[7] J.L.Shaffer, J.R.Petrella, F.C.Sheldon, K.R.Choudhury, V.D.Calhoun, R.E.Coleman, P.M.Doraiswamy and I.Alzheimer's Disease

Neuro- imaging; Radiology, **266(2)**, 583 **(2013)**.

[8] P.J.Toussaint, V.Perlbarg, P.Bellec, S.Desarnaud, L.Lacomblez, J.Doyon, M.O.Habert, H.Benali; Neuroimage, **63(2)**, 936 **(2012)**.

[9] S.Galluzzi, C.Geroldi, G.Amicucci, L.Bocchio Chiavetto, M.Bonetti, C.Bonvicini, M.Cotelli, R.Ghidoni, B.Paghera, O.Zanetti, G.B.Frisoni; Journal of Neurology, **260(2)**, 640 **(2013)**.

[10] M.Lopez, J.Ramirez, J.M.Gorriz, I.Alvarez, D.Salas-Gonzalez, F.Segovia, R.Chaves, P.Padilla, M.Gomez-Rio; Neurocomputing, **74(8)** 1260 **(2011)**.

[11] I.A.Illan, J.M.Gorriz, J.Ramirez, D.Salas- Gonzalez, M.M.Lopez, F.Segovia, R.Chaves, M.Gomez-Rio, C.G.Puntonet; Information Sciences, **181(4)**, 903 **(2011)**.

[12] X.L.Yuan, B.C.Shan, Y.C.Ma, J.H.Tian, K.D.Jiang, Q.Y.Cao, R.M.Wang; Journal of Alzheimers Disease, **19(3)**, 927 **(2010)**.

[13] W.L.Yang, R.L.M.Lui, J.H.Gao, T.F.Chan, S.T.Yau, R.A.Sperling, X.D.Huang; Journal of Alzheimers Disease, **27(1)**, 239 **(2011)**.

[14] K.J.Friston; Statistical parametric mapping: the analysis of funtional brain images, Amsterdam; Boston: Elsevier/Academic Press, **(2007)**.

[15] L.Xu, K.M.Groth, G.Pearlson, D.J.Schretlen, V.D.Calhoun; Hum Brain Mapp, **30(3)**, 711 **(2009)**.

[16] F.Fink, K.Worle, P.Gruber, A.M.Tome, J.M.Gorriz-Saez, C.G.Puntonet, E.W.Langof; ICA Analysis of Retina Images for Glaucoma Classification2008 at the 30th Annual International Conference of the IEEE Engineering in Medicine and Biology Society, **1**, 4664 **(2008)**.

[17] B.Magnin, L.Mesrob, S.Kinkingnehun, M.Pelegrini-Issac, O.Colliot, M.Sarazin, B.Dubois, S.Lehericy, H.Benali; Neuroradiology, **51(2)**, 73 **(2009)**.

[18] S.Kloppel, C.M.Stonnington, C.Chu, B.Draganski, R.I.Scahill, J.D.Rohrer, N.C.Fox, C.R.Jack, Jr., J.Ashburner, and R.S.Frackowiak; Brain, **131**, 681 **(2008)**.

[19] N.Correa, T.Adali, V.D.Calhoun; Magnetic Resonance Imaging, **25(5)**, 684 **(2007)**.

[20] J.Ashburner; Magnetic Resonance Imaging, **27(8)**, 1163 **(2009)**.

[21] V.Calhoun, T.Adali, L.K.Hansen, J.Larsen, J.Pekar; ICA of Functional MRI Data: An Overview at the 4th International Symposium on Independent Component Analysis and Blind Signal Separation (ICA2003), Nara, Japan, 1-4 Apr., **(2003)**.

[22] Y.O.Li, T.Adali, V.D.Calhoun; Human Brain Mapping, **28(11)**, 1251 **(2007)**.

[23] V.Calhoun, T.Adali, G.Pearlson, J.Pekar; Neuroimage, **13(6)**, S88 **(2001)**.

[24] C.W.Hsu, C.C.Chang, C.J.Lin; A Practical Guide to Support Vector, http://www.csie.ntu.edu.tw/~cjlin., **(2010)**.

[25] J.L.Lancaster, M.G.Woldorff, L.M.Parsons, M.Liotti, C.S.Freitas, L.Rainey, P.V.Kochunov, D.Nickerson, S.A.Mikiten, P.T.Fox; Human Brain Mapping, **10(3)**, 120 **(2000)**.

[26] D.Salas-Gonzalez, J.M.Gorriz, J.Ramirez, I.A.Illan, M.Lopez, M.Lopez, F.Segovia, R.Chaves, P.Padilla, C.G.Puntonet; Medical Physics, **37(11)**, 6084 **(2010)**.